Zoosyst. Evol. 100 (2) 2024, 543–553 | DOI 10.3897/zse.100.121238

PENSOFT

MUSEUM FÜR NATURKUNDE BERLIN

A new species of *Cyrenoida* (Bivalvia, Cyrenoididae) from the Western Atlantic, with remarks on Cyrenoididae anatomy

Bárbara L. Valentas-Romera[1], Luiz Ricardo L. Simone[1], Rodrigo Cesar Marques[2]

1 *Museu de Zoologia da Universidade de São Paulo, Laboratório de Malacologia, Avenida Nazaré, 481, CEP:04263–000, São Paulo, Brazil*

2 *Universidade Federal dos Vales do Jequitinhonha e Mucuri - Campus JK, Departamento de Ciências Biológicas (DCBio-FCBS), Rodovia MGT, 367, CEP 39100–000, Diamantina, Brazil*

https://zoobank.org/552EBECE-2FAB-4C54-8171-047763535D67

Corresponding author: Bárbara L. V. Valentas-Romera (barbarella.lou@gmail.com)

Academic editor: Thomas von Rintelen ♦ **Received** 20 February 2024 ♦ **Accepted** 3 April 2024 ♦ **Published** 14 May 2024

Abstract

Cyrenoida implexa **sp. nov.** is the first species of Cyrenoididae in the Southern West Atlantic. This new species exhibits external similarities to *C. floridana* but is distinguished by distinct right hinge dentition, larger siphons and a more extensive siphonal area at the mantle border, an incurrent siphon with three rows of papillae, a lack of papillae at the middle mantle fold, and smaller adductor muscle volume. In the environment, it possesses a higher saline tolerance than *C. floridana*.

Key Words

Anatomy, Bivalvia, *Cyrenoida*, Cyrenoididae, estuary, mangrove, taxonomy, Western Atlantic

Introduction

Mangroves and estuaries globally face numerous challenges (Lugo et al. 2014; Romañach et al. 2018). These environments have increasingly garnered attention, prompting extensive study and protection efforts. Consequently, public and political awareness of their economic, cultural, and social significance has heightened (Romañach et al. 2018; Moore et al. 2022). This increased attention has facilitated advancements in understanding the inhabitants of these unique environments.

In Brazil, studies on mangroves and estuaries have shed light on various topics, including litter (e.g. Duarte et al. 2023; Cavalcante et al. 2024), carbon storage (e.g. Mariano Neto et al. 2024), impacts of urbanization (e.g. Saad et al. 2019), and faunal distribution (e.g. Barroso and Matthews-Cascon 2009; Rodrigues et al. 2016). As anticipated, the advancement of these studies has resulted in the discovery of new species.

Cyrenoida Joannis, 1835, is a poorly known genus comprising six living species with infaunal filter-feeding habits that inhabit nutrient-rich sediments in the brackish waters of estuaries and mangroves across Western Africa, the Western Atlantic, the Eastern Pacific of North and Central America, and the Caribbean islands (Coan and Valentich-Scott 2012; Huber 2015; Valentas-Romera et al. 2019; Wu et al. 2023). Historically, this genus has been associated with lucinids, but recent phylogenetic studies have placed it within the Cyrenoididae, primarily consisting of species found in brackish, estuarine, or freshwater environments (Taylor et al. 2009; Lemer et al. 2019; Wu et al. 2023). Presently, the bulk of data on this taxon stems from a single species, *Cyrenoida floridana* Dall, 1896. However, *C. floridana* is restricted in distribution to North and Central America, the Caribbean, and Suriname, and is rare in scientific collections (Valentas-Romera et al. 2019).

With the goal of enhancing mollusk records along the Brazilian coast and advancing the understanding of taxonomy, morphology, and anatomy within *Cyrenoida*, a new species, *Cyrenoida implexa* sp. nov., is described based on shell and soft tissue data. Additionally, a brief comparison between the new species and *C. floridana* is conducted, expanding the morphological, anatomical, and physiological characterization of the genus and shedding light on new avenues for future research concerning this genus.

Methods

The specimens were initially identified as *Cyrenoida* sp. in Barroso and Matthews-Cascon (2009), Rodrigues et al. (2016), and Saad et al. (2019). Morphology of dry shells and anatomy of soft parts were studied using standard techniques (Valentas-Romera et al. 2019). All depictions of soft parts in this study are based on specimens from lots MZSP 99988 and MZSP 109105. Scanning electron microscopy (SEM) was provided by the Laboratório de Microscopia Eletrônica from the Museu de Zoologia of the Universidade de São Paulo.

The following abbreviations are used in the anatomical descriptions and figures: **aa:** anterior adductor muscle; **an:** anus; **ar:** anterior pedal retractor muscle; **au:** auricle; **cc:** cerebral connective; **cg:** cerebral ganglia; **cg:** cerebral ganglia; **dd:** digestive diverticula; **dg:** digestive gland; **dh:** dorsal hood; **dm:** dorsal siphonal retractor muscles; **eo:** excurrent opening; **er:** esophageal rim; **es:** esophagus; **ex:** excurrent siphon; **fg:** food groove; **fo:** esophageal folds; **fs:** F-shaped tooth **ft:** foot; **gf:** gill fusion; **gi:** gill; **go:** gonad; **gp**: genital pore; **gs:** gastric shield; **id:** inner demibranch; **if:** mantle border inner fold; **in:** intestine; **io:** incurrent opening; **ip:** inner palp; **ir:** inner row of siphonal papillae; **is:** incurrent siphon; **ki:** kidney; **lc:** left caecum; **li:** ligament; **lp**: left pouch; **lv:** inverted-V-shaped tooth; **mf:** mantle border middle fold; **mo:** mouth; **mr:** middle row of siphonal papillae; **mt:** major typhlosole; **np:** nephropore; **nt:** minor typhlosole; **od:** outer demibranch; **of:** mantle border outer fold; **op:** outer palp; **or:** outer row of siphonal papillae; **pa:** posterior adductor muscle; **pg:** pedal ganglia; **pl:** pallial line; **pm:** pallial muscle; **pp:** papillae; **pr:** posterior pedal retractor muscle; **rc:** right caecum; **sa1:** sorting area 1; **sa2:** sorting area 2; **sa3:** sorting area 3; **ss:** style sac; **st:** stomach; **t1:** large lateral tooth of right valve; **t2:** cardinal tooth of right valve; **t3:** small lateral tooth of right valve; **t4:** lateral tooth of left valve; **t5:** posterior cardinal tooth of left valve; **t6:** anterior cardinal tooth of left valve; **ub:** umbones; **ve:** ventricle; **vg:** visceral ganglia; **vm:** ventral siphonal retractor muscles.

Institutional abbreviations: **MZSP:** Museu de Zoologia da Universidade de São Paulo.

Results

Superfamily Cyrenoidea J. E. Gray, 1840
Family Cyrenoididae H. Adams & A. Adams, 1857 (1853)
Genus *Cyrenoida* Joannis, 1835

***Cyrenoida implexa* sp. nov.**

https://zoobank.org/B12440D9-ABCB-4A6B-8E8A-528C8C697ED3

Figs 1–23

Diplodonta punctata: Barroso and Matthews-Cascon 2009: 82–83 (non Say, 1822).

Cyrenoida sp.: Rodrigues et al. 2006: 395, 397; Huber 2015: 812; Saad et al. 2019: 5–6.

Types. *Holotype*: BRAZIL • specimen; MZSP 54637. Paratypes: 40 specimens; same locality as holotype; Barroso C.X. leg.;17 Oct.2005; MZSP 99988.

Type locality. BRAZIL. **Ceará**; Fortaleza, Ceará River estuary, Parque Soledade, 3°42'07.94"S, 38°36'36.22"W, IX Martins leg., 17.x.2005.

Extra material examined. BRAZIL • 1 specimen; **Maranhão**, São Luís, São Marcos Bay, Carangueijos Island, Igarapé mangrove; 2011; MZPS 100525. 2 specimens: **São Paulo**, São Vicente, Branco River mangrove; 23°56'17"S, 46°25'12"W; 2 Jul. 2011; Saad, L.O. leg.; MZSP 109103. 06 specimens; 08 Feb. 2012; Saad, L.O. leg; MZSP 109105. 2 specimens: Peruíbe, Una River mangrove, Ecological Station Juréia Itatins; 24°25'33"S, 47°05'05"W; 03 Apr.2012; Saad, L.O. leg; MZSP 109104.

Measurements (length, height, and maximum width in mm). MZUSP 54637: 7.2 by 7.3 by 4.3; MZSP 99988 #1: 7.1 by 6.9 by 4; #2: 8.2 by 8.3 by 4.5; #3: 6.7 by 6.6 by 3.6; #4: 6.7 by 6.2 by 3.4; #5: 4.9 by 4.6 by 2.9; #6: 5.4 by 5 by 3.1; #7: 6.8 by 6.3 by 3.4; #8: 6.1 by 5.5 by 3.3; #9: 5.5 by 5.3 by 3.3; MZSP 100525: 7.7 by 7.2 by 4.1.

Diagnosis. Shell rounded to subquadrate, posteriorly pointed; umbones high, thin; valves fragile; periostracum thin, light brown. Internal surface opaque; no nacreous aspect; no distinguishable muscular impression or pallial line. Hinge with laminar cardinal and lateral teeth; right hinge with inverse V-shaped tooth, formed by fusion between cardinal and lateral tooth; laminar, lateral tooth; left valve with recumbent F-shaped teeth, formed by fusion of two cardinal teeth and lateral tooth. Nymph is long and thin.

Description. Shell (Figs 1–7): Outline rounded to subquadrate, with ventral margin slightly posteriorly pointed. Width ~55% of shell length. External surface covered with well-marked growth lines. Equivalve, almost equilateral, ~5% longer than high, reaching maximum length of ~8 mm. Laterally inflated, width ~55% of total shell length. Externally white, adorned only by growth lines. Periostracum thin, light brown; slightly wrinkled at ventral shell margin (Figs 1, 2). Walls thin, fragile. Umbones central, prosogyre, low, ~6% of total shell height and ~27% of shell length, located almost at midpoint of shell length (Fig. 5). Internal surface opaque (Figs 3, 4). Muscle scars and pallial line almost imperceptible. Anterior adductor muscle scar reniform, occupying ~1.32% of total internal surface; twice higher than wide, located at mid third of shell height; Posterior adductor muscle scar oval, occupying ~1.49% of total internal surface; located at mid-third of shell height. Pallial line entire, away from shell margins ~8% of shell height. Hinge heterodont (Figs 6, 7): right valve with inverse V-shaped tooth (Fig. 7: lv), looking fusion between short cardinal tooth and long lateral tooth, with ~1% of total shell length and single laminar lateral tooth (Fig. 7: t3) located under inversed V-shaped tooth, ~38% longer than superior lateral tooth, forming groove between superior and inferior lateral teeth. Left valve with recumbent F-shaped tooth (Fig. 6: fs), forming ~90° angle, with bifid appearance, looking fusion of two cardinal tooth (t5, t6) at one lateral

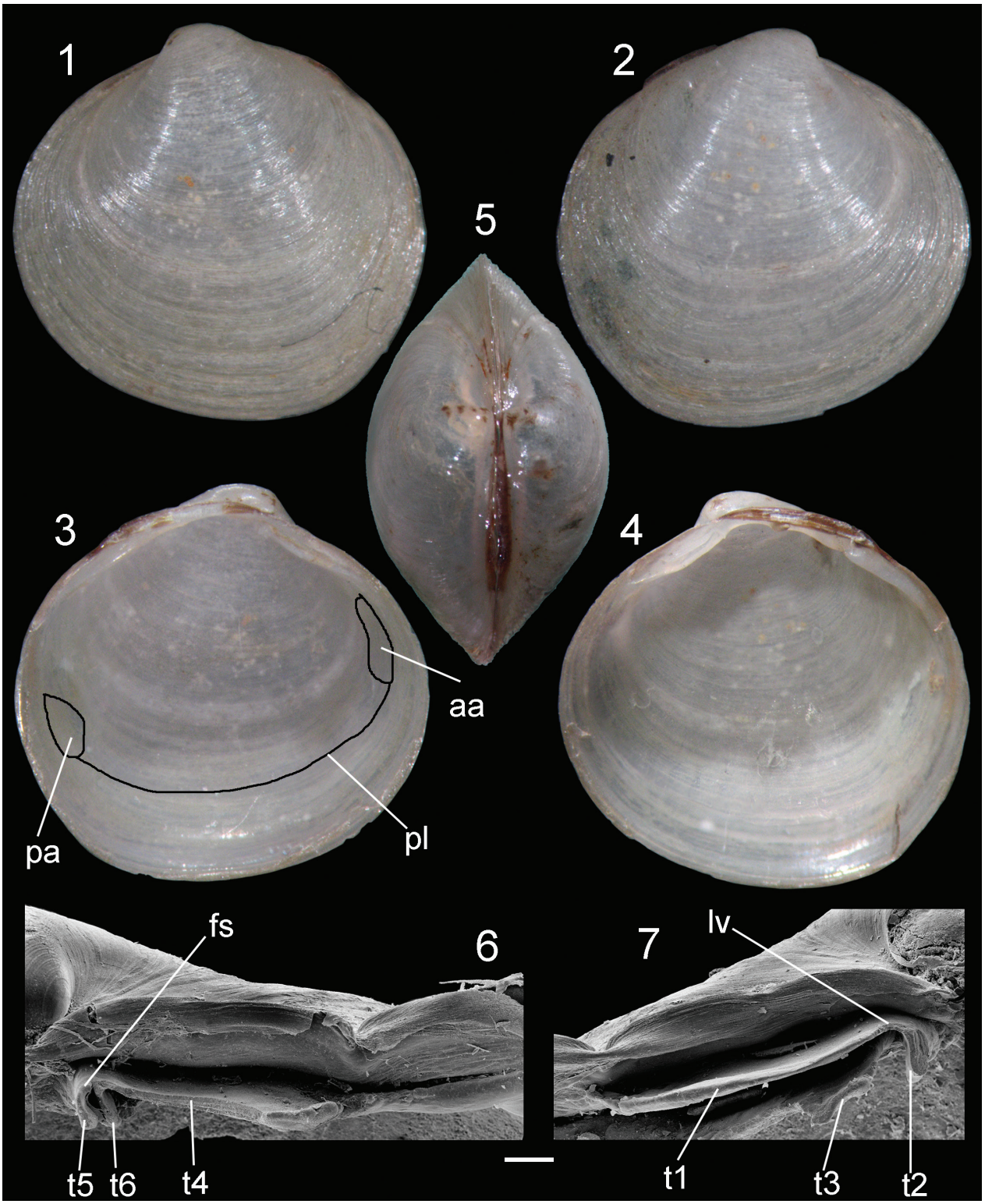

Figures 1–7. Holotype of *Cyrenoida implexa* sp. nov. (MZSP 54637, 7.2 mm, H 7.3 mm, W 4.3 mm). **1.** Left valve, outer view; **2.** Right valve, outer view; **3.** Left valve, inner view; **4.** Right valve, inner view; **5.** Whole dorsal view; **6.** Right hinge under SEM; **7.** Left hinge under SEM. Scale bar: 200 μm (**6, 7**).

tooth (t4). Dorsal margin concave. Ligament parvincular, opisthodetic, length ~40% of total shell length. Nymph ~9 times longer than wide, shape rhomboid. Lunule and escutcheon absent.

Main muscle system (Figs 8, 9, 13): Anterior adductor (aa) muscle reniform in transverse section, twice heigh than wide; ventral portion ~2.5 times wider than dorsal portion; occupying ~5% of total internal shell volume; located at median third of valve, clearly divided into quick and slow components, quick component occupying ~30% of anterior portion of muscle, dark grey in color, slow component occupying ~70% of posterior portion of muscle, light cream in color. Posterior adductor muscle (**pa**) elliptical in cross section, ~1.5 times wider than tall,

~30% shorter and ~1.3 times wider than anterior adductor muscle, located at opposite extremity of anterior adductor muscle, clearly divided into quick and slow components, the former occupying ~45% of posterior portion of muscle, dark gray in color, the latter occupying ~55% of anterior portion of muscle, light cream in color. Pair of foot anterior retractor muscles (ar) oval in section, thin, elongated; originated dorsally at anterior adductor muscle; running posteriorly and ventrally at ~20% of total shell length; both branches fusing at anterior edge of foot base. Pair of foot posterior retractor muscled (pr) oval in section, thin; originated dorsally at posterior adductor muscle; ~50% longer than pair of anterior retractors; both fusing posterior edge of foot base (Fig. 11). Two pairs of siphonal retractor muscles; dorsal siphonal retractors (dm) ~6 times longer than wide; insertion almost at central portion of mantle lobe, 2 times as long as excurrent opening, originating laterally at half of siphonal base height; ventral siphonal retractors (vm) thin, ~5 times longer than wide, length ~65% of total length of dorsal siphonal muscle, originating at ventral end of inhalant opening.

Foot and byssus (Figs 8, 11): Foot (ft) short; relaxed length ~50% of total shell height. Laterally flattened; end blunt, swollen. Foot base at median portion visceral sac. Byssus or byssal groove.

Mantle (Figs 8, 9, 11): Mantle lobes symmetrical, thin, translucent, colorless. Pallial muscles (pm) reunited in long muscles, distributed sparsely along ventral side of mantle lobe; height ~12% of total shell length, separated from each other by ~15 times pallial muscle basal width. Mantle edge trifolded (Fig. 9), unpigmented; outer fold (of) thick, ~7 times taller than wide; middle fold (mf) short, half of total outer fold height, same width; inner fold (if) short, length ~20% of outer fold height, ~30% of its width. Periostracum produced between external and middle fold. Mantle lobes totally free except for siphonal area. Anterior mantle fusion occurring at ~45% of anterior adductor muscle height; posterior mantle fusion occurring at ~68% of posterior adductor muscle height (Fig. 11). Siphonal area corresponding to ~42% of total mantle lobe length. Mantle lobes mostly free from each other, except for siphonal area, relative to 42% of mantle lobe total length (more details below).

Pallial cavity (Figs 8, 10–14, 16): Occupying about half of inner shell volume. Palps small, occupying ~30% of total shell volume. Pair of hemipalps triangular (Figs 11, 16), ~20% shorter but same width of insertion area of anterior adductor muscle; pair of external hemipalps (op) connected at mantle lobe by hemipalp dorsal border, in half of hemipalp length; pair of internal hemipalps (ip) connected at visceral mass by dorsal border, in ~30% of total hemipalp length. Internal surface of both palps covered by ~24 transverse folds; internal hemipalp folds high and rounded, covering ~90% of hemipalp internal surface, forming thin smooth area at hemipalp borders corresponding ~1% of total hemipalp internal area, folds decreasing towards mouth, forming shallow channels towards mouth (mo). Gills area ~30% of total valve area; outer demibranch (od) fusiform, twice longer than wide, folded on ~30% of total demibranch extension, covering pericardium and kidney areas, connected to mantle lobe by ~15% of total length of dorso posterior border of demibranch. Inner demibranch (id) triangular, ~twice longer than wide, folded on half of demibranch total extension, ~40% of internal demibranch area covered by external demibranch (Fig. 8); presenting food groove (fg); demibranchs connected to each other by tissue at posterior end, in ~20% of total gill length (Fig. 12). Suprabranchial chamber volume ~60% of infrabranchial chamber volume. Incurrent (is) and excurrent (ex) siphons originated by inner mantle fold; length ~30% of total shell length; each one ~3 times longer than wide in retracted condition; externally fused with each other; internally separated by thick, smooth muscular wall. Inner siphonal openings directly to pallial cavity (Figs 11, 14). Incurrent siphon length ~20% of total shell length, height ~1% of total shell height. Excurrent siphon length ~80% of inhalant siphon length; same width. Distal opening of incurrent siphon flanked by three rows of papillae (Fig. 14: ir, mr, or); papillae length equivalent ~5% of total inhalant siphon length. Distal opening of excurrent siphon with single row of flattened papillae (Fig. 14: 9p). Siphon attached to mantle by 2 pairs of muscle described above.

Visceral mass (Fig. 11): Visceral sac occupying half of inner shell volume; shape triangular. Slightly flattened; twice wider than muscular base; located dorsally at foot retractor muscles; ~20% of anterior portion filled with digestive diverticula of brown color; remaining areas with gonad of cream color. Stomach and style sac located vertically at central region.

Circulatory and excretory systems (Figs 11, 15, 23): Pericardium located dorsally in posterior half of visceral sac, between posterior portion of umbonal cavity and dorsal surface of kidney; twice longer than wide; occupying ~25% of total visceral sac volume. Pair of auricles (au) antero posteriorly long; connected to central axis of gill in ~30% of total auricle length; walls thin, translucent walls thin; located at central portion of pericardium; surrounding ~50% of intestinal portion crossing pericardium; connected to auricles in median portion of lateral walls. Kidney (ki) located postero ventrally at visceral mass (Figs 11, 15), below posterior end of pericardium and dorsal surface of posterior foot retractor muscles, color light brown; shape triangular, occupying ~25% of visceral mass volume. Gonopore (gp) rounded, located at posterior portion of visceral mass, at ~25% of visceral mass height, opening in suprabranchial chamber, next to nephropore (np).

Digestive system (Figs 16, 20–22): Palps and digestive diverticula described above. Mouth small, located in central portion at intersection of palps (Fig. 16), lips small. Esophagus (es) elongate, narrow, cylindric; length and height respectively ~16% and 1% of total visceral sac; no contact with anterior adductor muscle; passing through anterior portion of foot anterior retractors; internal surface with low longitudinal folds (fo); low esophageal rim (er) at stomach entrance; stomach (Figs 20–21: st) occupying

~25% of total visceral sac volume; shape elliptical, funnel-like; located slightly posteriorly to umbones; length ~80% of total visceral sac length, ~30% of visceral sac heigh; posterior portion ~60% wider than anterior portion. Paired apertures to digestive caeca located ventro-laterally of gastric anterior portion, in transition with esophagus; turned to ventral side of visceral sac. Dorsal hood (dh) narrow, thin, length ~25% of total stomach length, distally

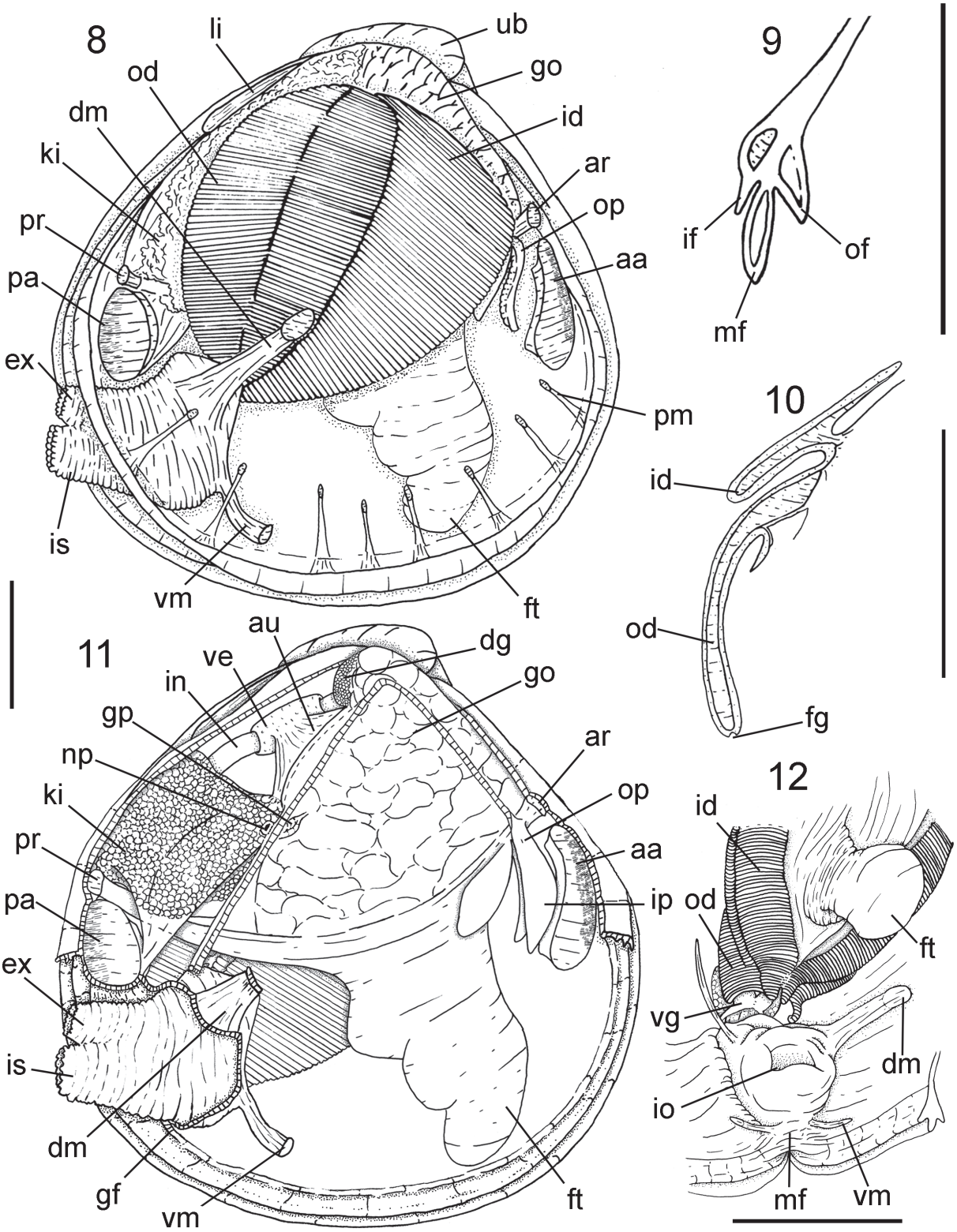

Figures 8–12. *Cyrenoida implexa*, anatomical drawings. **8.** Right view, valve removed, structures seen by transparency of mantle lobe; **9.** Mantle border, transverse section in its ventromedial portion; **10.** Gill, transverse section in its central portion; **11.** Right view, right mantle, and gill removed; **12.** Postero-ventral visceral region, ventral view, showing fusion of inner demibranchs in siphonal base and mantle fusion at siphonal area. Scale bars: 2 mm.

pointed. Left pouch (lp) located below anterior portion of dorsal hood, anteriorly to connection of digestive diverticula; shallow and wide; occupying ~20% of total area of left external wall of stomach. Internal surface of stomach (Fig. 22) mostly smooth, covered by three sorting areas well defined. First sorting area starting at left side of esophageal rim, running along dorsal wall of anterior stomach chamber, penetrating dorsal hood, narrow, comprised of small transverse folds (sa1). Second sorting area originating ventral to first sorting area, at left side of esophageal rim, running along left wall of anterior stomach chamber, entering left pouch and dorsal hood, both on their ventral surfaces, broad, formed by thickening of stomach wall (sa2). Third sorting area starting inside dorsal wall of dorsal hood, running along dorsal and right walls of posterior stomach chamber, until diffusing on ventral portion of right wall (sa3). Gastric shield (gs) located at central dorsal wall, occupying ~30% of total gastric area, with two anterior projections, one dorsal at left border, penetrating dorsal hood, and one left ventral, penetrating left pouch. Two narrow, tall gastric ridges running along ventral stomach chamber, forming major and minor typhlosoles at style sac opening. Longer ridge originating at ventral surface of stomach, surrounding left digestive diverticula, penetrating style sac at its right side, forming major typhlosole (mt). Shorter fold originating at style sac entrance, at region of major typhlosole penetration into style sac, forming rim bordering style sac entrance and

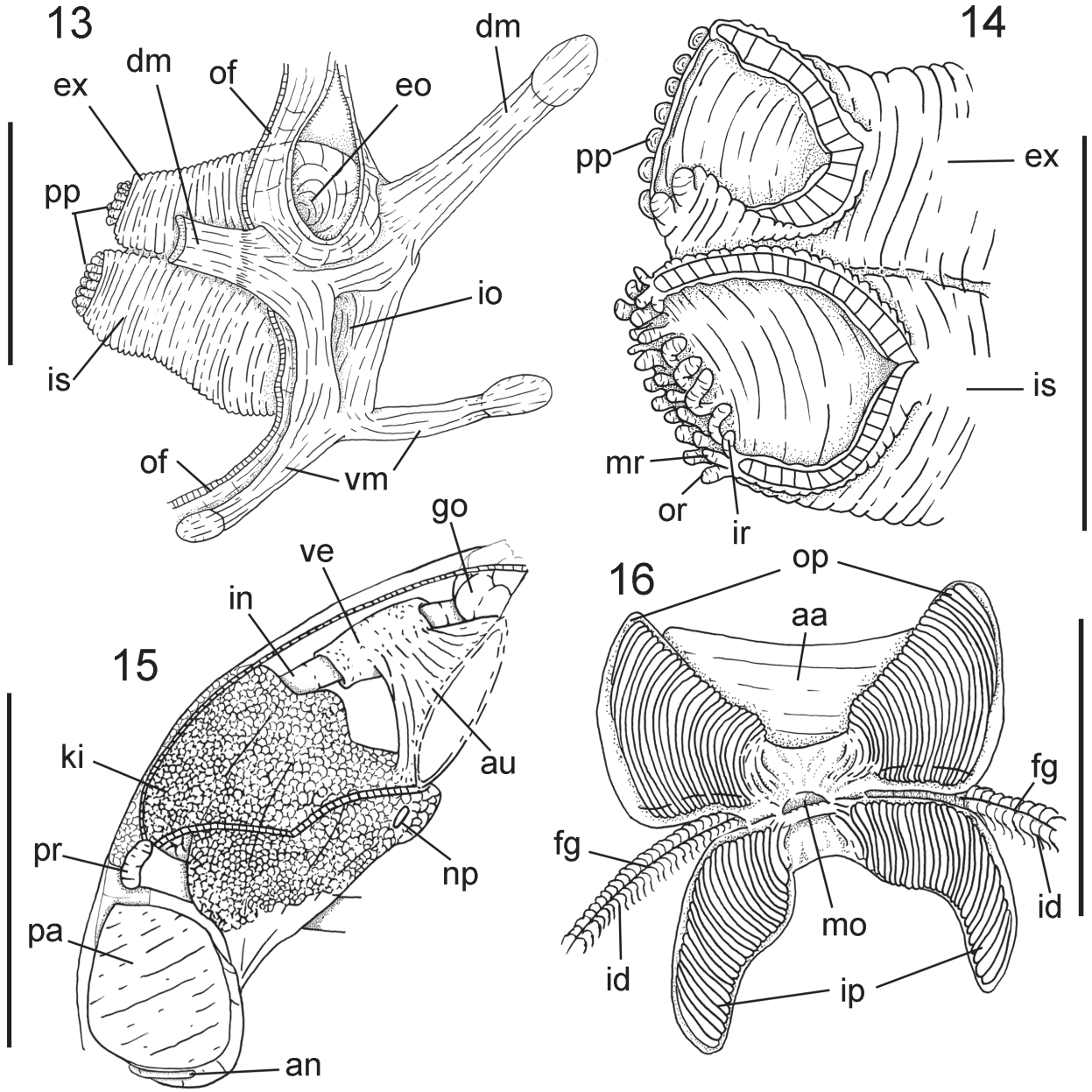

Figures 13–16. *Cyrenoida implexa* anatomical drawings. **13.** Incurrent and excurrent siphons, anterolateral view, right mantle lobe partially removed, some adjacent structures shown; **14.** Siphon tips; right view, both partially sectioned longitudinally; **15.** Pericardial region and kidney, right view, right mantle wall partially removed; **16.** Labial palps, ventral view, outer hemipalps deflected dorsally. Scale bars: 2 mm.

ultimately minor typhlosole (nt). Style sac (ss) connecting ventrally to dorsal portion of stomach; conical; tapering in ventral surface of visceral sac; ~3.5 times longer than wide; occupying ~16% of total visceral sac volume; height equivalent to half of visceral sac total length, length ~1% of visceral sac length. Intestine (in) narrow, long; starting in style sac; performing an inverted U-shaped loop under the anterior portion of the stomach, reaching the style sac high (Fig. 20), running towards dorso-posterior region of visceral sac parallel to style sac; leaving posterior portion of visceral sac, crossing pericardium and kidney; passing between posterior ends of foot posterior retractor muscles. Flanking entire posterior surface of posterior adductor muscle. Anus (an) on ventral surface of posterior adductor muscle; intestine total length ~9 times longer than style sac. Anus simple, sessile.

Genital system (Figs 11, 15): Gonads described above. Pair of gonoducts receiving sort of gonad acini along length along anterior portion of visceral sac. Genital pore simple, located at posterior region of visceral sac (Fig. 11: gp), opening next to nephropore (Figs 11, 15: np).

Central nervous system (Figs 17–19): Pair of cerebral ganglia (Fig. 17: cg) surrounding anterior dorsal half of esophagus, dorsally to labial palps; shape slightly triangular; longer than wide; size ~50% of esophagus width; cerebral commissure (cc) length ~60% of each ganglion length; from anterior portion connecting anterior adductor muscle nerve, bifurcating in two branches, internal branch

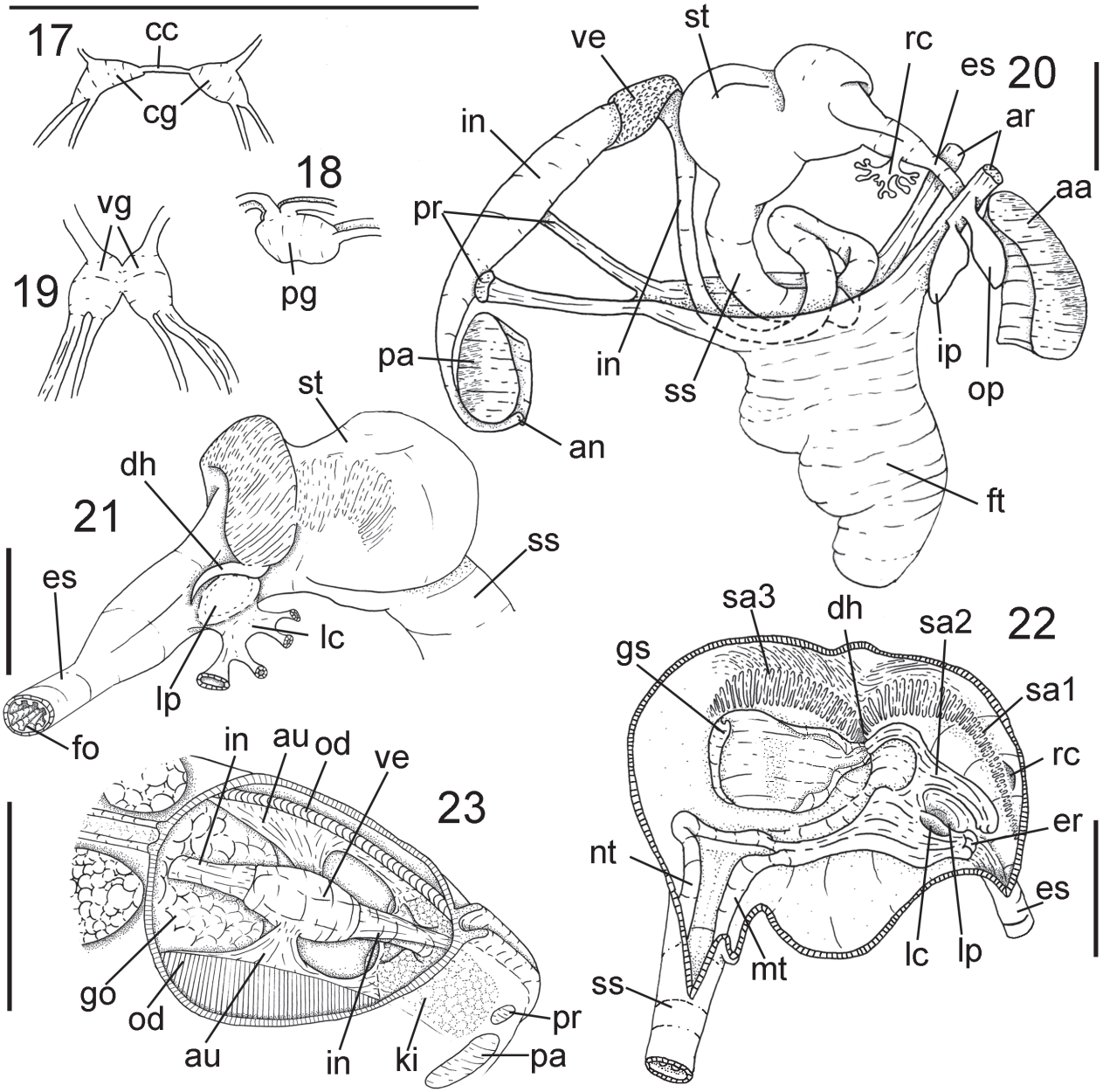

Figures 17–23. *Cyrenoida implexa* anatomical drawings. **17.** Cerebral ganglia, ventral view; **18.** Pedal ganglia, right view; **19.** Visceral ganglia, ventral view; **20.** digestive tubes and main musculature as in situ, right lateral view; **21.** stomach, left lateral view; **22.** Pericardial region, posterodorsal view, dorsal mantle wall partially removed; **23.** stomach, right lateral view, right wall opened and deflected to show inner gastric surface. Scale bars: 2 mm.

penetrating dorso posterior third of muscle and leaving at ventral surface of muscle; other branch bordering posterior surface of anterior muscle, both branches fusing at ventral region of anterior muscle; two connectives originating dorsally in ganglia, anteriorly to cerebro-visceral connective crossing visceral mass, touching gonopore dorsally, bordering anterior portion of kidney and connecting dorsally at visceral ganglia, connecting posteriorly cerebro-pedal connective running immersed at pedal muscles, connecting to anterior region of pedal ganglia. Pair of visceral ganglia (Fig. 19: vg) fusiform; each ganglion slightly longer than wide; ~80% of cerebral ganglia size; partially fused at median portion, with presence of shallow central groove; located ventrally at kidney, parallel to posterior adductor muscle; in dorsal tip connecting cerebra-visceral connective and renal nerve, penetrating into kidney area; laterally originating ctenidial nerves running thought central axis of posterior portion of gills; dorsally originating posterior adductor muscle nerve, penetrating median region of anterior surface of posterior muscle; at ventral tip originating pallial nerve, touching anterior surface of ventral portion of posterior adductor muscle, running parallel to inhalant and exhalant apertures and mantle border, diffusing at mantle lobe board. Pair of pedal ganglia (Fig. 18: pg) 40% larger than pair of cerebral ganglia; shape elliptic; longer than wide; totally fused with each other, without vestigial commissure; located immerse on foot retractor muscles, above foot insertion; in anterior tip connects cerebro-pedal connectives from cerebral ganglia; in posterior tip connecting two pairs of nerves, dorsal pair running towards posterior region inside posterior foot retractor muscles; postero-ventral nerves curved to ventral region, running internally.

Etymology. The specific epithet *implexa* is a Latin word for "tangled," referring to species commonly found between the roots of estuarine and mangrove plants.

Distribution. Brazil, Maranhão to São Vicente, São Paulo (Fig. 24).

Habitat. Mangroves in brackish water, buried until 15 cm in muddy sand.

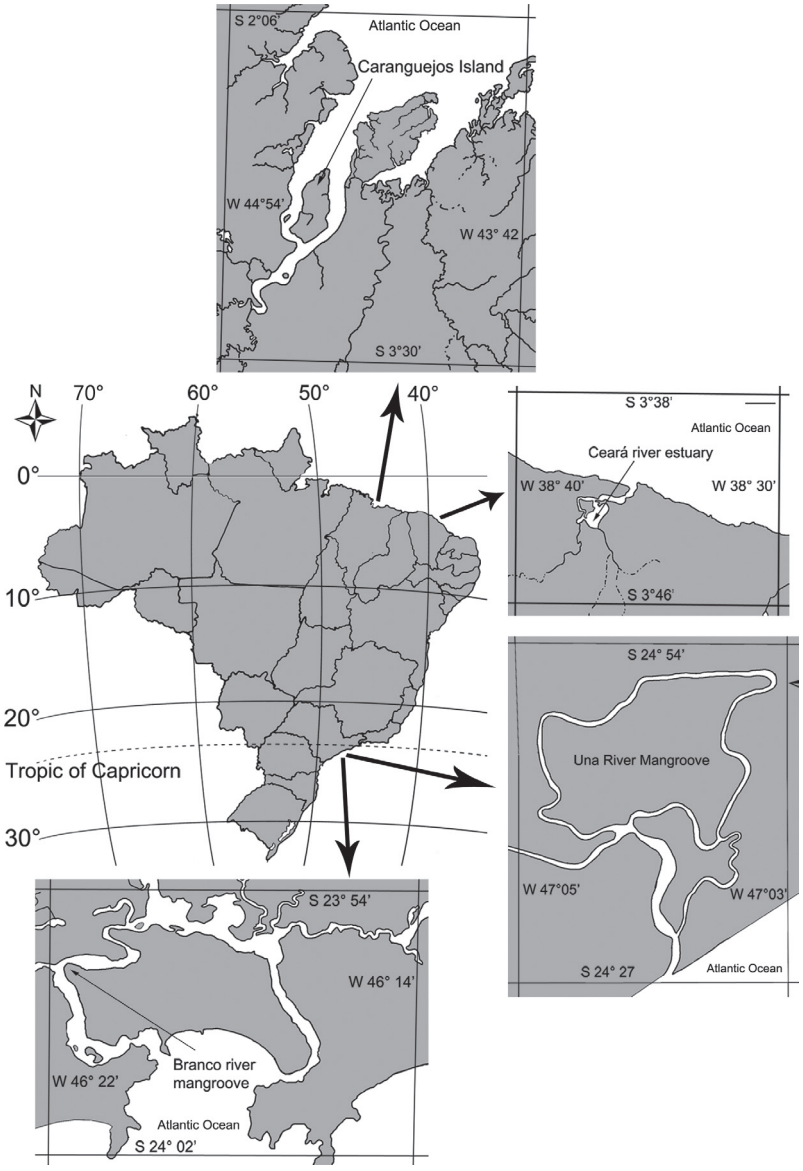

Figure 24. *Cyrenoida implexa* distribution along the Brazilian coast.

Discussion

At first glance, the external shell features of *C. implexa* closely resemble those of *Diplodonta punctata* (Say, 1822), which may strongly indicate misidentifications along the Brazilian coast (e.g., Barroso and Matthews-Cascon 2009). Both species exhibit rounded shells covered by a thin periostracum, displaying a light color, a posteriorly pointed shape, and living infaunally. Despite these initial similarities, differentiation differences between the two species are evident. *C. implexa* is found in estuaries and mangroves, featuring a slightly wrinkled and light brown periostracum (noticeable on dried specimens that retain it) and a fragile shell, while *D. punctata* inhabits a predominantly marine environment, burrowing into muddy or sandy bottoms, and possesses a hinge dentition composed exclusively of cardinal teeth (Mikkelsen and Bieler 2007; Rios 2009).

The classification of *C. implexa* within the genus *Cyrenoida* is primarily based on limited studies comparing it to *C. dupontia*, the type species of *Cyrenoida* (Joannis 1835; Deshayes 1836), as well as comments made on C. d'Ailly, 1869 (Taylor et al. 2009). These three species share several distinguishing features, including a hinge dentition characterized by fused laminar and cardinal teeth, the absence or faint presence of muscle scar impressions on the internal shell surface, valves covered with a brownish periostracum, a larger inner demibranch in the gills, paired triangular labial palps located at the anterior part of the ctenidia, and a pair of incurrent and excurrent siphons (Joannis 1835; Deshayes 1836; Taylor et al. 2009; Valentas-Romera et al. 2019). Furthermore, it is important to note the habitat of *C. implexa*, as these organisms are typically found thriving in freshwater to brackish environments, often intertwined among plant roots. Similar cyrenoidids with these characteristics are prevalent in both African and American ecosystems.

Most of the knowledge about the six *Cyrenoida* species stems from studies focusing on *C. floridana* in the Western Atlantic. Taylor et al. (2009), through molecular analysis of *C. floridana*, identified similarities among the families Cyrenoididae, Corbiculidae, and Glauconomidae. This finding led to the proposal of removing Cyrenoidindae from the superfamily Lucinoidea and assigning it to the superfamily Cyrenoidoidea, now known as Cyrenoidea. Subsequently, Wu et al. (2023) conducted another molecular analysis involving various *Cyrenoida* species, including *C. floridana*, and concluded that the family Cyrenoididae also encompasses *Geloina* J. E. Gray, 1842, *Cyanocyclas* Blainville, 1818, and *Polymesoda* Rafinesque, 1820.

Regarding *C. floridana* specifically, Valentas-Romera et al. (2019) undertook an extensive anatomical study comparing this species with others within Cyrenoidea, unveiling new morphological and anatomical insights, such as microtubules within shell walls, pairs of siphonal retractor muscles, the first description of the species' stomach, and evidence of shell parasitism in this species.

Given that additional studies involving the sequencing of *C. implexa* material are planned, the species is currently described based on its shell morphology and soft parts anatomy. These features are deemed comparable to those of *C. floridana*, as the available data is sufficiently convincing. Regarding the shell characters, both species are similar in outline and the characteristics of the left hinge teeth, especially the shape of the lateral tooth complex (t4) and cardinal teeth (t4 and t5). The studied specimens of *C. implexa* are also similar to *C. floridana* in size, as they fall within the species size range. The largest specimen documented in this study measures 8 mm, while *C. floridana* exhibits a length range of 10 to 14 mm (Valentas-Romera et al. 2019). Notably, reproductive populations of *C. floridana* described by Leathem et al. (1976), Kat (1982), and Wingard et al. (2022) include smaller individuals with average shell sizes of 9 mm, 3.5 to 4.5 mm, and less than 5 mm, respectively.

However, *C. implexa* and *C. floridana* can be differentiated by two sets of characteristics: a) right hinge teeth; b) internal anatomy; and c) ecological requirements.

a) The hinge in *C. implexa* is composed of three teeth: two lateral teeth, forming a single inverted V-shaped tooth, along with a solitary cardinal tooth (Fig. 1F, H). In contrast, *C. floridana* displays a different pattern with four teeth: two cardinal and two lateral teeth, creating two inverted V-shaped structures, where the smaller one is positioned beneath the larger one (Valentas-Romera et al. 2019). Notably, in *C. implexa*, only the larger or superior inverted V-shaped tooth (sv) is present, while the smaller one consists solely of the lateral tooth (t3) (Valentas-Romera et al. 2019).
b) Anatomically, *C. implexa* differs from *C. floridana* in the following features: the anterior and posterior adductor muscles in *C. implexa* are respectively ~12% and ~7% smaller than those in *C. floridana* (Valentas-Romera et al. 2019). However, this discrepancy in adductor muscle size could represent a specific trait or may be influenced by ontogenetic stages. *C. implexa* is also characterized by a sizable pair of siphons and a well-defined siphonal area at the mantle border. It also possesses a single pair of dorsal siphonal retractors muscles, whereas *C. floridana* has a smaller pair of dorsal siphonal retractors muscles, separated into two bundles (Valentas-Romera et al. 2019). Notably, *C. implexa* is further differentiated by the presence of three rows of papillae at the tip of the incurrent siphon and one row of papillae at the tip of the excurrent siphon. Additionally, the mantle borders of *C. implexa* lack papillae.
c) The salinity range of *C. floridana* varies from 0.25 to 20.7 practical salinity units (psu), while *C. implexa* tolerates salinities between 20.3 and 30 psu (Brewster-Wingard and Ishman 1999; Gaiser et al. 2006; Barroso and Matthews-Cascon 2009; Rodrigues et al. 2016; Saad et al. 2019; Wingard et al. 2022).

According to Wingard et al. (2022), *C. floridana* is a stenohaline species that inhabits oligohaline zones and can be used as an indicator of low-salinity environments. However, this feature apparently is not found in *C. implexa*, as samples were absent in Ceará´s river estuary, where the salinity was below 5 psu. This might indicate that *C. implexa* tolerates higher salinities than *C. floridana*.

The differentiation between both species is further substantiated by the consistent presence of these traits in all samples of *C. implexa* collected from the Brazilian coast, whereas the attributes of *C. floridana* remain uniform across Caribbean and North American samples. Given that the southernmost occurrence of *C. floridana* is observed on the coast of Guyanas (Valentas-Romera et al. 2019), it is plausible to suppose that the Amazon River Plume may have functioned as a reproductive barrier, as seen in mollusk groups (Giachini-Tosseto et al. 2022).

Conclusions

Based on the present findings, it is evident that the newly identified species, *Cyrenoida implexa* sp. n., is a member of the Cyrenoididae family. This species exhibits distinct morphological and anatomical characteristics in both shell morphology and soft parts anatomy, setting it apart from *C. floridana*. Furthermore, *Cyrenoida implexa* sp. n. represents the first documented record of the genus in the South region of the Western Atlantic, specifically in Brazilian mangroves and estuaries.

Acknowledgements

We thank Lara Guimarães (MZSP) for assistance with scanning electron microscopy; Luiza Saad (Instituto de Biociências da USP); Inês Xavier Martins (Universidade Federal Rural do Semi Árido); and Cristiane Xerez Barroso (Universidade Federal do Ceará) for granting material. This project was partly supported by Fapesp (Fundação de Amparo à Pesquisa) proc. #2010/11401–8 and CNPq (Conselho Nacional de Desenvolvimento Científico e Tecnológico) proc. #134425/2010–3, #159490/2012–0, and #203533/2014–3.

References

Adams H, Adams A (1853–1858) The Genera of Recent Mollusca: Arranged According to their Organization (Vol. 2). John van Voorst, London, 661 pp. https://doi.org/10.5962/bhl.title.4772

Barroso CX, Matthews-Cascon H (2009) Distribuição espacial e temporal da malacofauna no estuário do rio Ceará, Ceará, Brasil. Pan-American Journal of Aquatic Sciences 4: 79–86. https://panamjas.org/pdf_artigos/PANAMJAS_4(1)_79-86.pdf

Brewster-Wingard GL, Ishman SE (1999) Historical trends in salinity and substrate in central Florida Bay: A paleoecological reconstruction using modern analogue data. Estuaries 22(2): 369–383. https://doi.org/10.2307/1353205

Cavalcante ER, Ribeiro VV, Taddei RR, Castro IB, Alves MJ (2024) High levels of anthropogenic litter trapped in a mangrove area under the influence of different uses. Marine Pollution Bulletin 200: 116045. [ISSN 0025–326X] https://doi.org/10.1016/j.marpolbul.2024.116045

Coan EV, Valentich-Scott P (2012) Bivalve Seashells of Tropical West America – Marine Bivalve Mollusks from Baja California to Northern Peru (2 vols). Santa Barbara Museum of Natural History, Santa Barbara, 1258 pp.

Deshayes M (1836) Sur la cyrénoide de M. de Joannis. Suivie d'une lettre de M. Joannis. (Cl. V, n°64). Magasin de Zoologie 6, Classe V: 1–3. https://biodiversitylibrary.org/page/2633064

Duarte LFA, Ribeiro RB, Medeiros TV, Scheppis WR, Gimiliani GT (2023) Are mangroves hotspots of marine litter for surrounding beaches? Hydrodynamic modeling and quali-quantitative analyses of waste in southeastern Brazil. Regional Studies in Marine Science 67: 103177. [ISSN 2352–4855] https://doi.org/10.1016/j.rsma.2023.103177

Gaiser EE, Zafiris A, Ruiz PL, Tobias FAC, Ross MS (2006) Tracking rates of ecotone migration due to salt-water encroachment using fossil mollusks in coastal south Florida. Hydrobiologia 569(1): 237–257. https://doi.org/10.1007/s10750-006-0135-y

Giachini-Tosseto E, Bertrand A, Neumann-Leitão S, Nogueira-Júnior M (2022) The Amazon River plume, a barrier to animal dispersal in the Western Tropical Atlantic. Scientific Reports 12(1): 537. https://doi.org/10.1038/s41598-021-04165-z

Gray JE (1840) Shells of molluscous animals. In: British Museum (Ed.) Synopsis of the contents of the British Museum. ed 42. G Woodfall, London, 105–152. https://www.biodiversitylibrary.org/page/55287672

Huber M (2015) Compendium of Bivalves 2. A Full-Color Guide to the Remaining Seven Families. A Systematic Listing of 8'500 Bivalve Species and 10'500 Synonyms. ConchBooks, 907 pp.

Joannis [L.] De (1835) Cyrénoide. *Cyrenoida*. Joannis. Magasin de Zoologie 5. Classe V, 2 pp. [pl. 64] https://www.biodiversitylibrary.org/page/37121825

Kat PW (1982) Reproduction in a peripheral population of *Cyrenoida floridana* (Bivalvia, Cyrenoididae). Malacologia 23(1): 47–54. https://biodiversitylibrary.org/page/13112410

Leathem W, Kinner P, Mauer D (1976) Northern range extension of the Florida marsh clam *Cyrenoida floridana* (superfamily Cyrenoidacea). The Nautilus 90(3): 93–94. https://biodiversitylibrary.org/page/8276463

Lemer S, Bieler R, Giribet G (2019) Resolving the relationships of clams and cockles: dense transcriptome sampling drastically improves the bivalve tree of life. Proceedings of the Royal Society B: Biological Sciences 286(1896): 1–9. https://doi.org/10.1098/rspb.2018.2684

Lugo AE, Medina E, McGinley K (2014) Issues and challenges of mangroves conservation in the Anthropocene. Madera y Bosques 20: 11–38. https://doi.org/10.21829/myb.2014.200146

Mariano Neto M, da Silva JB, de Brito HC (2024) Carbon stock estimation in a Brazilian mangrove using optical satellite data. Environmental Monitoring and Assessment 196(9): 9. https://doi.org/10.1007/s10661-023-12151-3

Mikkelsen PM, Bieler R (2007) Seashells of Southern Florida: Living Marine Mollusks of the Florida Keys and Adjacent Regions. Bivalves. Princetion University Press, Princeton, New Jersey, 503 pp. https://doi.org/10.1515/9780691239453

Moore AC, Hierro L, Mir N, Stewart T (2022) Mangrove cultural services and values: Current status and knowledge gaps. People and culture 4: 1083–1097. https://doi.org/10.1002/pan3.10375

Rios EC (2009) Compendium of Brazilian Sea Shells. Rio Grande, RS,668 pp.

Rodrigues CA, Ribeiro RP, Santos NB, Almeida ZS (2016) Patterns of mollusc distribution in mangroves from the São Marcos Bay, coast of Maranhão State, Brazil. Acta Amazonica 46(4): 391–400. https://doi.org/10.1590/1809-4392201600493

Romañach SS, DeAngelis DL, Koh HL, Li Y, Teh SY, Raja Barizan RS, Zhai L (2018) Conservation and restoration of mangroves: Global status, perspectives, and prognosis. Ocean and Coastal Management 154(15): 72–82. https://doi.org/10.1016/j.ocecoaman.2018.01.009

Saad LO, Cunha CM, Colpo KD (2019) How mollusk assemblages respond to different urbanization levels: Characterization of the malacofauna in subtropical Brazilian mangroves. Marine Biodiversity 49(2): 989–999. https://doi.org/10.1007/s12526-018-0883-8

Say T (1822) An account of some of the marine shells of the United States. Journal of the Academy of Natural Sciences of Philadelphia 2: 302–325. https://www.biodiversitylibrary.org/item/113421#page/318/mode/1up

Taylor JD, Glover EA, Williams ST (2009) Phylogenetic position of the bivalve family Cyrenoididae – removal from (and further dismantling of) the superfamily Lucinoidea. The Nautilus 123(1): 9–13. https://biodiversitylibrary.org/page/50438173

Valentas-Romera BL, Simone LRL, Mikkelsen PM, Bieler R (2019) Anatomical redescription of *Cyrenoida floridana* (Bivalvia, Cyrenoididae) from the Western Atlantic and its position in the Cyrenoidea. Zoosystematics and Evolution 95(2): 517–534. https://doi.org/10.3897/zse.95.38456

Wingard GL, Stackhouse BL, Daniels AM (2022) Using mollusks as indicators of restoration in nearshore zones of south Florida's estuaries. Bulletin of Marine Science 98(3): 351–380. https://doi.org/10.5343/bms.2022.0004

Wu R, Liu L, Liu X, Ye Y, Wu X, Xie Z, Liu Z, Li Z (2023) Towards a systematic revision of the superfamily Cyrenoidea (Bivalvia, Imparidentia): Species delimitation, multi-locus phylogeny and mitochondrial phylogenomics. Invertebrate Systematics 37(9): 607–622. https://doi.org/10.1071/IS23015